Research Square

Preprints are preliminary reports that have not undergone peer review.
They should not be considered conclusive, used to inform clinical practice,
or referenced by the media as validated information.

Development and External Validation of a Predictive Model for Epithelial Ovarian Tumors Based on MRI Features and Serum Tumor Markers

Zhi Li
Huzhou Women and Children's Hospital
Zhongfeng Niu
Sir Run Run Shaw Hospital
Linghong Qi
Huzhou Women and Children's Hospital
Shuiying Mao
Huzhou Women and Children's Hospital
Pengfei Wang
wangpengfei00011@163.com
Huzhou Women and Children's Hospital

Article

Keywords: Ovarian tumors, Magnetic resonance imaging, Prediction model human epididymis protein 4, carbohydrate antigen 125

Posted Date: June 1st, 2026

DOI: https://doi.org/10.21203/rs.3.rs-9433115/v1

License: This work is licensed under a Creative Commons Attribution 4.0 International License. Read Full License

Additional Declarations: No competing interests reported.

Version of Record: A version of this preprint was published at Scientific Reports on November 1st, 2026. See the published version at https://doi.org/10.1038/s41598-026-79217-3.

Abstract

Ovarian cancer remains a major threat to women's health, and early-stage disease often lacks specific clinical manifestations, making timely diagnosis challenging. Early and accurate preoperative assessment is essential for improving patient outcomes.To develop and externally validate a predictive model integrating magnetic resonance imaging (MRI) features and serum tumor markers for distinguishing benign from malignant epithelial ovarian tumors. A total of 222 patients from Huzhou Maternity & Child Health Care Hospital constituted the training cohort, and 102 patients from Sir Run Run Shaw Hospital, Zhejiang University School of Medicine formed the external validation cohort. Independent risk factors for ovarian cancer were identified using multivariate binary logistic regression. A predictive model was then constructed based on the weighted regression coefficients of these factors and subsequently validated in an external cohort. In the training cohort, 168 patients (183 lesions) were benign and 54 patients (68 lesions) were malignant. Multivariate analysis identified tumor morphology, diffusion-weighted imaging (DWI) signal intensity, presence of ascites, carbohydrate antigen 125 (CA125), and human epididymis protein 4 (HE4) as independent predictors of malignancy, with AUCs of 0.755, 0.887, 0.749, 0.830, and 0.803, respectively. The combined predictive model achieved an AUC of 0.966, with a sensitivity of 89.6% and specificity of 89.7%. Calibration analysis demonstrated good agreement (Hosmer–Lemeshow test, P = 0.777).In the external validation cohort, 80 patients (87 lesions) were benign and 22 patients (28 lesions) were malignant. The model achieved an AUC of 0.949, with a sensitivity of 96.6% and specificity of 89.3%. The proposed model integrating MRI features and serum tumor markers demonstrated excellent diagnostic performance and robust external validity. This practical and easily applicable tool may assist in preoperative risk stratification and clinical decision-making.

Introduction

Ovarian cancer is one of the most common gynecologic malignancies, approximately 90% of which are epithelial in origin. Globally, more than 300,000 new cases are diagnosed annually, with approximately 152,000 related deaths each year (1). It remains the leading cause of mortality among gynecologic malignancies worldwide (2, 3).Due to the absence of specific symptoms in the early stages, nearly 70% of patients are diagnosed at an advanced stage, where the 5-year survival rate ranges from 20% to 36%. In contrast, early-stage detection is associated with a 5-year survival rate of up to 90% (4). Therefore, accurate early diagnosis and timely intervention are essential to improve clinical outcomes.

Previous studies have primarily focused on ultrasound-based assessment (5, 6), serum tumor markers (7, 8), or their combined application (9) for the prediction of ovarian tumors. In contrast, magnetic resonance imaging (MRI) based predictive models remain relatively underexplored (10, 11), and most available studies are limited to descriptive analyses of imaging features rather than quantitative risk modeling with external validation.

In the present study, we systematically analyzed clinical variables, Magnetic resonance imaging (MRI) features, and serum tumor markers in patients with epithelial ovarian tumors to develop an integrated preoperative predictive model for differentiating benign from malignant lesions. The model's diagnostic performance and generalizability were further assessed using an independent external validation cohort. We aimed to enhance preoperative diagnostic accuracy and provide a practical tool to support individualized clinical decision-making and treatment planning.

Materials and Methods

Paricipants

Stuy Population

The training cohort comprised patients who underwent surgical resection for epithelial ovarian tumors at Huzhou Maternal and Child Health Care Hospital between October 2021 and October 2025. Clinical data were retrieved from the electronic medical record system, and MRI images were obtained from the institutional Picture Archiving and Communication System (PACS).Inclusion criteria were as follows:(1)Complete clinical data available;(2)Preoperative multiparametric MRI performed with clearly identifiable lesions and images of diagnostic quality;(3)No prior treatment before MRI examination;(4)Postoperative histopathological confirmation of epithelial ovarian tumor. Exclusion criteria were:(1)Histopathological diagnosis of borderline ovarian tumor;(2)Coexistence of two different types of malignant tumors.

Patients with histopathologically confirmed benign epithelial ovarian tumors were assigned to the benign group, whereas those with malignant epithelial ovarian tumors were assigned to the malignant group. Ultimately, 168 patients (183 lesions) were included in the benign group and 54 patients (68 lesions) in the malignant group.

This retrospective study was approved by the Ethics Committees of Huzhou Maternity & Child Health Care Hospital and Sir Run Run Shaw Hospital, Zhejiang University School of Medicine (Approval Nos. 2023-R-025 and 2026-2056-01). All procedures performed in this study involving human participants were in accordance with the ethical standards of the institutional research committees and with the 1964 Helsinki Declaration and its later amendments.The requirement for written informed consent was waived due to the retrospective study design.

MRI examination method

MRI examinations were performed using 1.5-T scanners in both cohorts. The training cohort was scanned with a Siemens Avanto 1.5T system (Siemens Healthcare, Erlangen, Germany), whereas the validation cohort was examined using a Siemens Sonata 1.5T system (Siemens Healthcare, Erlangen, Germany).Routine imaging parameters were as follows: slice thickness, 5 mm; interslice gap, 1.5 mm; field of view (FOV), 380 × 380 mm^2; and number of excitations (NEX), 2.The imaging protocol included the following sequences:Axial T2-weighted imaging (T2WI): TR 3,000–4,500 ms; TE 70–90 ms; Coronal T2WI: TR 3,000–4,000 ms; TE 80–110 ms; Sagittal T2WI: TR 3,000–4,500 ms; TE 70–90 ms; Axial T1-weighted imaging (T1WI): TR 500–800 ms; TE 10–20 ms; Sagittal T1WI: TR 500–800 ms; TE 10–20 ms; Axial diffusion-weighted imaging (DWI): TR 2,000–4,000 ms; TE 70–100 ms. For contrast-enhanced imaging, a gadolinium-based contrast agent (gadodiamide) was administered intravenously at a dose of 0.1 mmol/kg body weight. Contrast-enhanced axial and sagittal T1WI sequences were acquired using the same parameters as the pre-contrast scans.

Clinical and Laboratory Data Collection

Clinical variables collected included patient age, duration of symptoms, and menopausal status.

Laboratory data comprised serum tumor markers, including carbohydrate antigen 19-9 (CA19-9), carcinoembryonic antigen (CEA), alpha-fetoprotein (AFP), carbohydrate antigen 125 (CA125), and human epididymis protein 4 (HE4). All participants underwent preoperative collection of 3 mL of fasting peripheral venous blood. Blood samples were centrifuged at 3,500 rpm for 10 minutes (centrifugal radius, 10 cm), and the serum was carefully separated for analysis. Serum tumor marker levels were measured using the Abbott ARCHITECT i2000SR (Abbott Laboratories, USA) according to the manufacturer's instructions.

MRI Image Analysis

All MRI examinations were independently reviewed by two radiologists with 11 and 9 years of experience in pelvic MRI interpretation, respectively. Both readers were blinded to the histopathological results and clinical information. In cases of discrepancy, a third senior radiologist with 20 years of experience in pelvic MRI evaluated the images, and a consensus was reached.

The following imaging features were assessed:lesion laterality (unilateral or bilateral), maximum lesion diameter, tumor morphology, margin characteristics, tumor composition (cystic, cystic-solid, or solid), presence of mural nodules, septal thickness, signal intensity on T1WI, signal intensity on T2WI, signal intensity on DWI; b = 1000 s/mm^2), arterial-phase enhancement rate, venous-phase enhancement rate, short-axis diameter of the largest pelvic lymph node, presence of ascites.

Tumor composition was categorized as follows (12): cystic (< 1/3 solid component), cystic-solid (1/3–2/3 solid component), and solid (> 2/3 solid component). Signal intensities on T1WI and T2WI were evaluated relative to the iliopsoas muscle. Septal thickness was measured at the thickest portion on T2WI. Ascites was defined as the presence of intraperitoneal fluid after excluding patients with clinically confirmed cirrhosis, pelvic inflammatory disease, pelvic tuberculosis, or other known causes of non-malignant effusion.

Measurement of Contrast Enhancement Rate

For quantitative assessment of contrast enhancement, a circular region of interest (ROI) measuring 20–40 mm^2 was manually placed within the solid component of the lesion, carefully avoiding necrotic, cystic, or hemorrhagic areas. Signal intensity (SI) values were measured on the same imaging slice at the following phases: pre-contrast, arterial phase, and venous phase.

Each SI measurement was performed three times, and the mean value was recorded for analysis.The arterial-phase enhancement rate was calculated as:"Arterial enhancement rate"=(SI_(arterial)-SI_(precontrast))/(SI_(precontrast)). The venous-phase enhancement rate was calculated as:"Venous enhancement rate"=(SI_(venous)-SI_(precontrast))/(SI_(precontrast))

Construction of the Predictive Model

Each candidate variable was initially evaluated using univariate analysis. Variables with a P value < 0.05 were subsequently entered into a multivariate binary logistic regression model to identify independent predictors of malignant epithelial ovarian tumors. Multivariate analysis was performed using a backward stepwise selection method based on the likelihood ratio test. Independent predictors identified in the final model were retained. A predictive model was constructed based on the regression coefficients (β) derived from the multivariate logistic regression analysis.

External Validation

The predictive model developed in the training cohort was subsequently applied to an independent external validation cohort. The validation cohort consisted of consecutive patients with surgically and histopathologically confirmed epithelial ovarian tumors treated at Sir Run Run Shaw Hospital, Zhejiang University School of Medicine, between November 2023 and October 2025. The inclusion and exclusion criteria were identical to those applied in the training cohort. A total of 102 patients (115 lesions) were included in the validation cohort, comprising 80 patients (87 lesions) with benign epithelial ovarian tumors and 22 patients (28 lesions) with malignant epithelial ovarian tumors.

Statistical Analysis

All statistical analyses were performed using SPSS software (version 22.0; IBM Corp., Armonk, NY, USA) and MedCalc (version XX; MedCalc Software Ltd., Ostend, Belgium). Continuous variables were tested for normality using the Shapiro–Wilk test. Normally distributed data are presented as mean ± standard deviation (SD) and were compared using the independent-samples t test. Non-normally distributed data are expressed as median with interquartile range and were compared using the Mann–Whitney U test. Categorical variables are presented as frequencies and percentages and were compared using the chi-square test or Fisher's exact test, as appropriate.

Variables with P < 0.05 in univariate analysis were entered into a multivariate binary logistic regression model to identify independent predictors. Odds ratios with 95% confidence intervals were calculated. Receiver operating characteristic (ROC) curve analysis was used to calculate the area under the curve (AUC). The optimal cutoff value was determined using the Youden index. Model calibration was assessed using the Hosmer–Lemeshow goodness-of-fit test.

All statistical tests were two-tailed, and a *P* value < 0.05 was considered statistically significant

Results

Comparison of Clinical Characteristics, MRI Features, and Tumor Markers Between the Two Groups in the Training Cohort

In the training cohort, univariate analysis demonstrated significant differences between the benign and malignant groups in tumor location, margin characteristics (regular vs. irregular), tumor composition, DWI signal intensity, arterial-phase enhancement rate, venous-phase enhancement rate, short-axis diameter of the largest pelvic lymph node, presence of ascites, serum CA125 level, and HE4 level (all *P* < 0.05). Detailed results are summarized in Table 1.

Multivariate Logistic Regression Analysis of Epithelial Ovarian Tumors

Variables with *P* < 0.05 in the univariate analysis were entered into a multivariate binary logistic regression model to identify independent predictors of malignancy. Tumor malignancy (benign vs. malignant epithelial ovarian tumor) was defined as the dependent variable. The candidate independent variables included tumor location, morphology, tumor composition, DWI signal intensity, arterial-phase enhancement rate, venous-phase enhancement rate, short-axis diameter of the largest pelvic lymph node, presence of ascites, serum CA125 level, and HE4 level.

Multivariate analysis revealed that irregular tumor morphology, high signal intensity on DWI, presence of ascites, elevated CA125, and elevated HE4 were independently associated with malignant epithelial ovarian tumors (all P < 0.05). The corresponding odds ratios with 95% confidence intervals are presented in Table 2.

Development and Performance Evaluation of the Combined Predictive Model

The diagnostic performance of each independent predictor was evaluated using ROC curve analysis, and the corresponding AUC are presented in Fig. 1.

A combined predictive model was constructed based on the regression coefficients (β) derived from the multivariate logistic regression analysis. To facilitate clinical application and simplify score calculation, the smallest regression coefficient (CA125) was normalized to a weight of 1, and the remaining coefficients were proportionally scaled according to their relative magnitudes.

The final predictive formula was defined as:
Combined predictive score=393.5×(irregular morphology)+619.75×(high DWI signal)+405.75×(ascites)+1×(CA125)+4.75×(HE4).Binary variables were coded as 0 (absent) and 1 (present). The combined model demonstrated excellent discriminatory ability, with an AUC of 0.966 (Fig. 2). Model calibration was assessed using the Hosmer–Lemeshow goodness-of-fit test, which indicated good calibration ($\chi^2 = 4.821$, df = 8, $P = 0.777$), suggesting adequate agreement between predicted and observed probabilities of malignancy.

The diagnostic performance metrics of each independent predictor and the combined model, including AUC, sensitivity, specificity, and Youden index, are summarized in Table 3.

External Validation of the Combined Predictive Model

The external validation cohort consisted of patients with surgically and histopathologically confirmed epithelial ovarian tumors treated at Sir Run Run Shaw Hospital, Zhejiang University School of Medicine, between November 2023 and October 2025. A total of 102 patients (115 lesions) were included, comprising 80 patients (87 lesions) with benign tumors and 22 patients (28 lesions) with malignant tumors. In the external cohort, the combined predictive model demonstrated favorable discriminatory performance, with an area under the ROC curve (AUC) of 0.949 (Fig. 3). The sensitivity, specificity, and Youden index were 96.6%, 89.3%, and 0.859, respectively. These results suggest that the model maintains good diagnostic performance in an independent cohort, supporting its potential generalizability.

Discussion

Ultrasound is widely used as the first-line imaging modality for the evaluation of ovarian tumors because of its accessibility, cost-effectiveness, and convenience (13). However, its diagnostic performance is highly operator-dependent, and it may be limited in accurately characterizing complex lesions and comprehensively assessing the pelvic cavity (14). MRI owing to its superior soft-tissue contrast resolution, enables detailed characterization of ovarian masses and precise delineation of adjacent pelvic structures. In addition, its noninvasive nature and multiplanar capability facilitate comprehensive pelvic assessment (15). MRI is therefore considered the most accurate noninvasive imaging modality for differentiating benign from malignant ovarian tumors (16, 17).

Morphological characteristics of ovarian tumors provide important information for lesion characterization (18). Benign tumors typically exhibit a smooth and well-defined contour, whereas malignant tumors more frequently demonstrate irregular morphology.

In the present study, univariate analysis showed that irregular morphology was observed in 55.9% (38/68) of malignant lesions, which was significantly higher than in benign lesions (4.9%, 9/183; P < 0.05). Multivariate logistic regression further identified irregular morphology as an independent predictor of malignancy, with an AUC of 0.755.

Several pathophysiological mechanisms may explain this association. Malignant tumors generally exhibit rapid and disorganized proliferation, leading to heterogeneous growth patterns and uneven tumor contours. In addition, infiltrative growth into adjacent tissues may contribute to irregular tumor margins (19). Rapid proliferation can also result in relative ischemia, causing necrosis, hemorrhage, and cystic degeneration, thereby increasing internal structural complexity and distorting overall morphology. Furthermore, exophytic growth patterns observed in certain malignant tumors may further accentuate contour irregularity.

DWI enables the evaluation of tissue signal alterations following the application of diffusion-sensitizing gradients, thereby reflecting the microstructural characteristics of lesions (20). By exploiting differences in water molecule diffusivity across tissues, DWI assists in distinguishing benign from malignant tumors. Compared with conventional MRI sequences, DWI provides additional functional information related to tissue cellularity and membrane integrity. As a noninvasive imaging technique, it indirectly reflects alterations in water mobility and tumor microenvironment characteristics, thereby offering incremental value in the preoperative assessment of ovarian tumors. With advances in functional MRI techniques, including DWI, the diagnostic performance for ovarian tumors has improved substantially (21, 22). In the present study, DWI demonstrated a sensitivity of 84.7% and a specificity of 92.6% for predicting ovarian malignancy. The sensitivity was comparable to that reported in a previous meta-analysis (86.0%), whereas the specificity was slightly higher than the pooled estimate of 81.0% (23). One potential explanation is that the meta-analysis included non-neoplastic conditions such as endometriosis, which may exhibit high signal intensity on DWI and consequently reduce specificity. In contrast, endometriosis was not included in our study cohort, which may partially account for the relatively higher specificity observed.

Ascites refers to the pathological accumulation of fluid within the peritoneal cavity, resulting from increased fluid production or impaired absorption, often related to enhanced vascular permeability and lymphatic obstruction (24). In ovarian malignancies, ascites is commonly associated with advanced-stage disease and unfavorable prognosis (25-27). Previous studies have reported that more than one-third of patients with ovarian cancer develop ascites (28).

In the present study, the incidence of ascites in the malignant group was 59.3% (32/54), which appears higher than previously reported rates. One potential explanation may be differences in diagnostic criteria. In earlier studies, the minimum volume threshold for defining ascites was not clearly specified. In contrast, in our study, after excluding alternative causes such as liver cirrhosis, pelvic inflammatory disease, and pelvic tuberculosis, the presence of any detectable peritoneal fluid on imaging was classified as ascites-positive. This definition is consistent with that adopted by Ozyilmaz et al. (11). Multivariate analysis further identified ascites as an independent predictor of ovarian malignancy, with an AUC of 0.749. These findings suggest that the presence of ascites may reflect more aggressive tumor biology, potentially related to peritoneal dissemination, tumor-induced vascular permeability, and impaired lymphatic drainage.

Previous studies have shown that during tumor development and metastasis, both tumor cells and surrounding stromal cells secrete biomolecules that reflect malignant biological activity; these substances are collectively referred to as tumor markers (29). Due to their convenience, minimal invasiveness, and relatively low cost, serum tumor markers are widely used in clinical practice for the detection and monitoring of ovarian tumors.

CA125 remains the most commonly used biomarker in ovarian cancer. Serum CA125 plays an important role in the evaluation of ovarian masses, and dynamic changes in CA125 levels may reflect treatment response and disease progression (30). Zhang et al. (31) reported that CA125 is useful for assessing chemotherapy response and prognosis in ovarian cancer. However, approximately 50% of patients with early-stage ovarian cancer do not exhibit elevated CA125 levels, which limits its sensitivity in early detection. Consequently, CA125 is often combined with other biomarkers to improve diagnostic performance (32-34). HE4 is a relatively novel biomarker that is overexpressed in a substantial proportion of ovarian cancers (35). Unlike CA125, HE4 levels are not significantly influenced by the menstrual cycle. Previous studies have demonstrated that although the sensitivity of HE4 is comparable to that of CA125, its specificity is generally higher (36, 37). In addition, HE4 is minimally expressed in normal ovarian tissue and most benign ovarian tumors, which enhances its discriminatory ability (38). Winarno et al. (39) identified CA125 as an independent predictor of ovarian cancer, while Braicu et al. (40) reported that HE4 is an independent prognostic factor.

In the present study, both CA125 and HE4 were identified as independent predictors of ovarian malignancy, with AUC values of 0.830 and 0.803, respectively. Although each biomarker demonstrated moderate diagnostic performance individually, their integration into the combined predictive model substantially improved overall discrimination. The complementary biological characteristics of CA125 and HE4 may partially account for their enhanced diagnostic value when used in combination.

The MRI features of epithelial ovarian tumors and serum tumor markers are biologically heterogeneous and reflect different aspects of tumor behavior. Therefore, reliance on a single parameter is unlikely to provide comprehensive diagnostic discrimination between benign and malignant ovarian tumors. Each individual predictor has inherent limitations that may restrict overall diagnostic accuracy.

In the present study, among the five independent predictors identified, DWI demonstrated the highest specificity (92.6%), whereas the remaining predictors showed maximum specificities of 70.6%. Although DWI exhibited relatively strong discriminatory performance,

the moderate specificity of the other variables may increase the likelihood of false-positive findings, underscoring the limitations of single-parameter assessment. In contrast, integration of these variables into a multivariable model substantially improved overall diagnostic performance. The combined model achieved a sensitivity of 89.6% and a specificity of 89.7%, with a Youden index exceeding that of any individual predictor. The AUCs for tumor morphology, DWI signal intensity, ascites, CA125, and HE4 were 0.755, 0.887, 0.749, 0.830, and 0.803, respectively, whereas incorporation into the combined model increased the AUC to 0.966, indicating excellent discriminatory capacity. Calibration analysis using the Hosmer–Lemeshow goodness-of-fit test demonstrated satisfactory agreement between predicted and observed outcomes, supporting model reliability. Importantly, external validation further confirmed model stability, yielding an AUC of 0.949, sensitivity of 96.6%, specificity of 89.3%, and a Youden index of 0.859. These findings suggest that the integrated imaging–biomarker model provides superior diagnostic discrimination compared with any single predictor.

From a clinical perspective, the improved balance between sensitivity and specificity achieved by the combined model may reduce both missed malignancies and unnecessary surgical procedures, thereby enhancing its potential value in preoperative risk stratification and decision-making.

Although the proposed predictive model demonstrated favorable diagnostic performance, several limitations should be acknowledged. First, the sample size was relatively limited, with an imbalance between benign and malignant cases. This distribution may introduce potential selection bias and increase the risk of overfitting. Although both internal and external validations showed consistent performance, larger multicenter studies with a more balanced representation of malignant tumors are needed to further confirm the robustness and generalizability of the model. Second, DWI was assessed qualitatively based on signal intensity rather than quantitatively using apparent diffusion coefficient (ADC) measurements. Qualitative evaluation may be influenced by interobserver variability and subjective interpretation. Incorporation of quantitative ADC parameters in future studies may provide more objective and reproducible diffusion metrics, thereby potentially enhancing model stability and performance. Finally, this was a retrospective study, which may inherently introduce selection bias and limit control over confounding variables. Prospective validation in independent cohorts would further strengthen the clinical applicability of the model. Despite these limitations, the findings support the feasibility of integrating MRI features and serum biomarkers into a combined predictive framework and warrant further prospective validation.

By integrating clinical characteristics, MRI features, and serum tumor markers, we developed and externally validated a combined predictive model for differentiating benign from malignant epithelial ovarian tumors. The model demonstrated high diagnostic accuracy, good calibration, and consistent performance across independent cohorts.

This combined model offers a practical approach for preoperative assessment and may assist clinicians in more accurately stratifying patients with epithelial ovarian tumors.

Declarations

Authors' contributions

All authors contributed to the study conception and design. Material preparation and data collection were performed by Zhi Li, Zhongfeng Niu, Linghong Qi, Shuiying Mao and Pengfei Wang. Data analysis was performed by Zhi Li, Linghong Qi, and Shuiying Mao. The first draft of the manuscript was written by Zhi Li and Zhongfeng Niu, and all authors commented on previous versions of the manuscript. All authors read and approved the final manuscript.

Funding

This work was supported in part by the Huzhou Science and Technology Plan of Zhejiang Province (2023GYB61)

Competing interests

The authors declare no competing interests.

Data Availability

All data supporting the findings of this study are available within the paper and its Supplementary Information.

References

1. Bray, F. et al. Global Cancer Statistics 2022: Globocan Estimates of Incidence and Mortality Worldwide for 36 Cancers in 185 Countries. *CA. Cancer. J. Clin.* **74**,229-263. https://doi.org/10.3322/caac.21834 (2024).
2. Lheureux, S., Gourley, C., Vergote, I., Oza, A.M. Epithelial Ovarian Cancer. *Lancet.* **393**,1240-1253. https://doi.org/10.1016/s0140-6736(18)32552-2(2019).
3. Morgan, R.J. et al. Ovarian Cancer, Version 1.2016, Nccn Clinical Practice Guidelines in Oncology. J *Natl. Compr. Canc. Netw.* **14**,1134-1163. https://doi.org/ 10.6004/jnccn.2016.0122 (2016).
4. Webb, P.M., Jordan, S.J. Epidemiology of Epithelial Ovarian Cancer. *Best. Pract. Res. Clin. Obstet. Gynaecol.* **41**,3-14. https://doi.org/10.1016/j.bpobgyn.2016.08.006 (2017).
5. Miao, K. et al. Prediction of Benign and Malignant Ovarian Tumors Using Resnet34 on Ultrasound Images. *J. Obstet. Gynaecol. Res.* **49**,2910-2917. https://doi.org/10.1111/jog.15788 (2023).
6. Suryawanshi, S.V., Dwidmuthe, K.S., Savalkar, S., Bhalerao, A. Diagnostic Efficacy of Ultrasound-Based International Ovarian Tumor Analysis Simple Rules and Assessment of the Different Neoplasias in the Adnexa Model in Malignancy Prediction among Women with Adnexal Masses: A Systematic Review. *Cureus.* **16**,e67365. https://doi.org/10.7759/cureus.67365 (2024).
7. Spagnol, G. et al. Clinical Utility and Diagnostic Accuracy of Roma, Rmi, Adnex, He4, and Ca125 in the Prediction of Malignancy in Adnexal Masses. *Cancers.* **16**. https://doi.org/10.3390/cancers16223790 (2024).
8. Oranratanaphan, S., Wanishpongpan, S., Termrungruanglert, W., Triratanachat, S. Assessment of Diagnostic Values among Ca-125, Rmi, He4, and Roma for Cancer Prediction in Women with Nonfunctional Ovarian Cysts. *Obstet. Gynecol. Int.* **2018**,7821574. https://doi.org/10.1155/2018/7821574 (2018).
9. Bahadur, A. et al. Comparison of Human Epididymis Protein 4, Cancer Antigen 125, and Ultrasound Prediction Model in Differentiating Benign from Malignant Adnexal Masses. *J. Midlife. Health.* **14**,176-183. https://doi.org/10.4103/jmh.jmh_77_23 (2023).
10. Li, H. et al. Diffusion-Weighted Magnetic Resonance Imaging and Morphological Characteristics Evaluation for Outcome Prediction of Primary Debulking Surgery for Advanced High-Grade Serous Ovarian Carcinoma. *J. Magn. Reson. Imaging.* **57**,1340-1349. https://doi.org/10.1002/jmri.28418 (2023).
11. Ozyilmaz, S., Kulali, F., Topal, C.S., Yalcinkaya, C. Salient Magnetic Resonance Imaging Findings in the Differential Diagnosis of Benign, Borderline and Malignant Ovarian Mucinous Tumors. *Abdom. Radiol. (NY).* **50**,1009-1017.https://doi.org/10.1007/s00261-024-04545-9 (2025).
12. Liu, L. et al. A Prediction Nomogram for Suboptimal Debulking Surgery in Patients with Serous Ovarian Carcinoma Based on Mri T1 Dual-Echo Imaging and Diffusion-Weighted Imaging. *Insights. Imaging.* **13**,204. https://doi.org/10.1186/s13244-022-01343-z (2022).
13. Campbell, S., Gentry-Maharaj, A. The Role of Transvaginal Ultrasound in Screening for Ovarian Cancer. *Climacteric.* **21**,221-226. https://doi.org/10.1080/13697137.2018.1433656 (2018).
14. Denewar, F.A. et al. Multiparametric Mri for Differentiation of Borderline Ovarian Tumors from Stage I Malignant Epithelial Ovarian Tumors Using Multivariate Logistic Regression Analysis. *Eur. J. Radiol.* **91**,116-123. https://doi.org/10.1016/j.ejrad.2017.04.001 (2017).
15. Thomassin-Naggara, I. et al. Characterization of Complex Adnexal Masses: Value of Adding Perfusion- and Diffusion-Weighted Mr Imaging to Conventional Mr Imaging. *Radiology.* **258**,793-803. https://doi.org/ 10.1148/radiol.10100751 (2011).
16. Sadowski, E.A., Robbins, J.B., Rockall, A.G., Thomassin-Naggara, I. A Systematic Approach to Adnexal Masses Discovered on Ultrasound: The Adnex Mr Scoring System. *Abdom. Radiol. (NY).* 43(3):679-695. https://doi.org/10.1007/s00261-017-1272-7 (2018).
17. Sadowski, E.A. et al. O-Rads Mri Risk Stratification System: Guide for Assessing Adnexal Lesions from the Acr O-Rads Committee. *Radiology.* **303**,35-47. https://doi.org/10.1148/radiol.204371 (2022).
18. Tamai, K. et al. The Utility of Diffusion-Weighted Mr Imaging for Differentiating Uterine Sarcomas from Benign Leiomyomas. *Eur. Radiol.* **18**,723-730. https://doi.org/10.1007/s00330-007-0787-7 (2008).

19. Santoro, A. et al. The Multiple Facets of Ovarian High Grade Serous Carcinoma: A Review on Morphological, Immunohistochemical and Molecular Features. *Crit. Rev. Oncol. Hematol.* **208**,104603. https://doi.org/10.1016/j.critrevonc.2024.104603 (2025).
20. Gagliardi, T., Adejolu, M., deSouza, N.M. Diffusion-Weighted Magnetic Resonance Imaging in Ovarian Cancer: Exploiting Strengths and Understanding Limitations. *J. Clin. Med.* **11**. https://doi.org/10.3390/jcm11061524 (2022).
21. deSouza, N.M., Rockall, A., Freeman, S. Functional Mr Imaging in Gynecologic Cancer. *Magn. Reson. Imaging. Clin. N. Am.* **24**,205-222. https://doi.org/ 10.1016/j.mric.2015.08.008 (2016).
22. Addley, H., Moyle, P., Freeman, S. Diffusion-Weighted Imaging in Gynaecological Malignancy. *Clin. Radiol.* **72**,981-990. https://doi.org/10.1016/j.crad.2017.07.014 (2017).
23. Yuan, X., Guo, L., Du, W., Mo, F., Liu, M. Diagnostic Accuracy of Dwi in Patients with Ovarian Cancer: A Meta-Analysis. *Medicine. (Baltimore).* **96**,e6659. https://doi.org/10.1097/md.0000000000006659 (2017).
24. Geng, Z., Pan, X., Xu, J., Jia, X. Friend and Foe: The Regulation Network of Ascites Components in Ovarian Cancer Progression. *J. Cell. Commun. Signal.* **17**,391-407. https://doi.org/10.1007/s12079-022-00698-8 (2023).
25. Worzfeld, T. et al. The Unique Molecular and Cellular Microenvironment of Ovarian Cancer. *Front. Oncol.* **7**:24. https://doi.org/10.3389/fonc.2017.00024 (2017).
26. Brencicova, E. et al. Interleukin-10 and Prostaglandin E2 Have Complementary but Distinct Suppressive Effects on Toll-Like Receptor-Mediated Dendritic Cell Activation in Ovarian Carcinoma. *PloS. one.* **12**,e0175712. https://doi.org/10.1371/journal.pone.0175712 (2017).
27. Saini, U. et al. Elevated Stat3 Expression in Ovarian Cancer Ascites Promotes Invasion and Metastasis: A Potential Therapeutic Target. *Oncogene.* **36**,168-181. https://doi.org/10.1038/onc.2016.197 (2017).
28. Kipps, E., Tan, D.S., Kaye, S.B. Meeting the Challenge of Ascites in Ovarian Cancer: New Avenues for Therapy and Research. *Nat. Rev. Cancer.* **13**,273-82. https://doi.org/10.1038/nrc3432 (2013).
29. Dochez, V., Caillon, H., Vauce, E., Dimet, J., Winer, N, Ducarme, G. Biomarkers and Algorithms for Diagnosis of Ovarian Cancer: Ca125, He4, Rmi and Roma, a Review. *J. Ovarian. Res.* **12**,28. https://doi.org/10.1186/s13048-019-0503-7 (2019).
30. Babic, A. et al. Predictors of Pretreatment Ca125 at Ovarian Cancer Diagnosis: A Pooled Analysis in the Ovarian Cancer Association Consortium. *Cancer. Causes. Control.* **28**,459-468. https://doi.org/ 10.1007/s10552-016-0841-3 (2017).
31. Zhang, M., Cheng, S., Jin, Y., Zhao, Y., Wang, Y. Roles of Ca125 in Diagnosis, Prediction, and Oncogenesis of Ovarian Cancer. *Biochim. Biophys. Acta. Rev. Cancer.* **1875**,188503. https://doi.org/10.1016/j.bbcan.2021.188503 (2021).
32. Zhang, R., Siu, M.K.Y., Ngan, H.Y.S., Chan, K.K.L. Molecular Biomarkers for the Early Detection of Ovarian Cancer. *Int. J. Mol. Sci.* **23**. https://doi.org/ 10.3390/ijms231912041 (2022).
33. Elias, K.M., Guo, J., Bast, R.C. J.r. Early Detection of Ovarian Cancer. *Hematol. Oncol. Clin. North. Am.* **32**,903-914.https://doi.org/10.1016/j.hoc.2018.07.003 (2018).
34. Cviič, D. et al. A Dual Biomarker Tk1 Protein and Ca125 or He4-Based Algorithm as a Better Diagnostic Tool Than Roma Index in Early Detection of Ovarian Cancer. *Cancers.* **15**. https://doi.org/10.3390/cancers15051593 (2023).
35. Feng, P., Chen, T., Wischhusen, J., Ladbury, C., Vargas-Hernández, V.M, Xiong, Y. The Diagnostic Performance of the Mindray System in Detecting Ca125 and He4 for Patients with Ovarian Cancer. *Transl. Cancer. Res.* **13**,4474-4484. https://doi.org/10.21037/tcr-24-1107 (2024).
36. Yu, C., Dou, T., Liu, Y., Liu, R. Clinical Value of Tv-Cds Combined with Serum Tumor Markers in Diagnosis of Ovarian Cancer. *Oncol. Lett.* **20**,2028-2034. https://doi.org/ 10.3892/ol.2020.11705 (2020).
37. Carreras-Dieguez, N. et al. Comparison of He4, Ca125, Roma and Cph-I for Preoperative Assessment of Adnexal Tumors. *Diagnostics. (Basel).* **12**. https://doi.org/10.3390/diagnostics12010226 (2022).
38. Kim, B. et al. Diagnostic Performance of Ca 125, He4, and Risk of Ovarian Malignancy Algorithm for Ovarian Cancer. *J. Clin. Lab. Anal.* **33**,e22624. https://doi.org/10.1002/jcla.22624 (2019).
39. Winarno, G.N.A. et al. Nomogram Development for Predicting Ovarian Tumor Malignancy Using Inflammatory Biomarker and Ca-125. *Sci. Rep.* **14**,15790. https://doi.org/10.1038/s41598-024-66509-9 (2024).
40. Braicu, EI. et al. Preoperative He4 Expression in Plasma Predicts Surgical Outcome in Primary Ovarian Cancer Patients: Results from the Ovcad Study. *Gynecol. Oncol.* **128**,245-251. https://doi.org/ 10.1016/j.ygyno.2012.11.023 (2013).

Tables

Table 1 Comparison of Clinical Characteristics, MRI Features, and Tumor Markers Between the Two Groups in the Training Cohort

Clinical Characteristics and MRI Features	Benign	Malignant	Statistical Value	*P* value
Age	49.81±17.52	51.87±11.31	1.089	0.278
Postmenopausal	78	25	0.000	0.986
Premenopausal	90	29		
Unilateral	153	38	14.576	<0.001
Bilateral	15	16		
Lesion Length(*cm*)	6.50（4.10~10.20）	6.35（5.05~10.08）	0.232	0.817
Regular Morphology	174	30	84.613	<0.001
Irregular Morphology	9	38		
Cystic Lesion	154	11	147.156	<0.001
Cystic-solid Lesion	24	47		
Solid Lesion	5	10		
Papillary Wall Nodule Present	43	22	2.026	0.155
No Papillary Wall Nodule	140	46		
Septal Thickness(*mm*)	2.232±0.95	2.30±0.86	0.328	0.743
Solid T1 Hypointensity	100	35	5.245	0.073
Isosignal on T1	80	28		
Hyperintensity on T1	3	5		
Solid T2 Hypointensity	60	16	3.769	0.152
Isosignal on T2	114	45		
Hyperintensity on T2	9	7		
DWI Isosignal	155	5	128.338	<0.001
DWI Hyperintensity	28	63		
Arterial Phase Enhancement Rate	0.5（0.30~1.00）	1.15（0.90~1.38）	5.797	<0.001
Venous Phase Enhancement Rate	0.7（0.40~1.30）	1.30（0.90~1.60）	4.116	<0.001
Long Axis of Lymph Node(mm)	0.40（0.40~0.50）	0.50（0.40~0.58）	1.370	0.171
Ascites Present	19	32	53.096	<0.001
No Ascites	149	22		
CA199	7.00（3.45~16.55）	10.60（4.40~21.40）	1.581	0.114
CEA	1.60（1.20~2.30）	1.50（1.20~2.38）	0.069	0.945
AFP	2.4（1.70~3.49）	2.46（1.90~3.14）	0.530	0.596
CA125	14.20（10.30~21.90）	136.25（22.55~378.20）	8.045	<0.001
HE4	36.40（29.40~46.50）	126.15（46.73~245.25）	7.367	<0.001

Table 2 Multivariate Logistic Regression Analysis of Epithelial Ovarian Tumors

Variable	B Value	Standard Deviation	Wald X^2 Value	OR (95% CI)	*P* Value
Irregular Shape	1.574	0.698	5.07	4.824（1.228~18.952）	0.024
DWI High Signal	2.479	0.722	11.783	11.934（2.897~49.163）	＜0.001
Ascites	1.623	0.597	7.392	5.067（1.573~16.322）	0.007
CA125	0.004	0.002	5.675	1.004（1.001~1.007）	0.17
HE4	0.019	0.006	10.024	1.019（1.007~1.031）	0.002

Table 3 Diagnostic Performance of Individual Risk Factors and the Combined Predictive Model for Ovarian Epithelial Tumors

	Sensitivity	Specificity	Youden index	Cut off value	AUC
Tumor morphology	95.1%	55.9%	0.510	-	0.755
DWI	84.7%	92.6%	0.773	-	0.887
Ascites	88.0%	61.8%	0.498	-	0.749
CA125	95.6%	66.2%	0.618	43.9	0.830
HE4	91.3%	70.6%	0.619	66.7	0.803
Combined Predictive Model	89.6%	89.7%	0.793	810.25	0.966

Figures

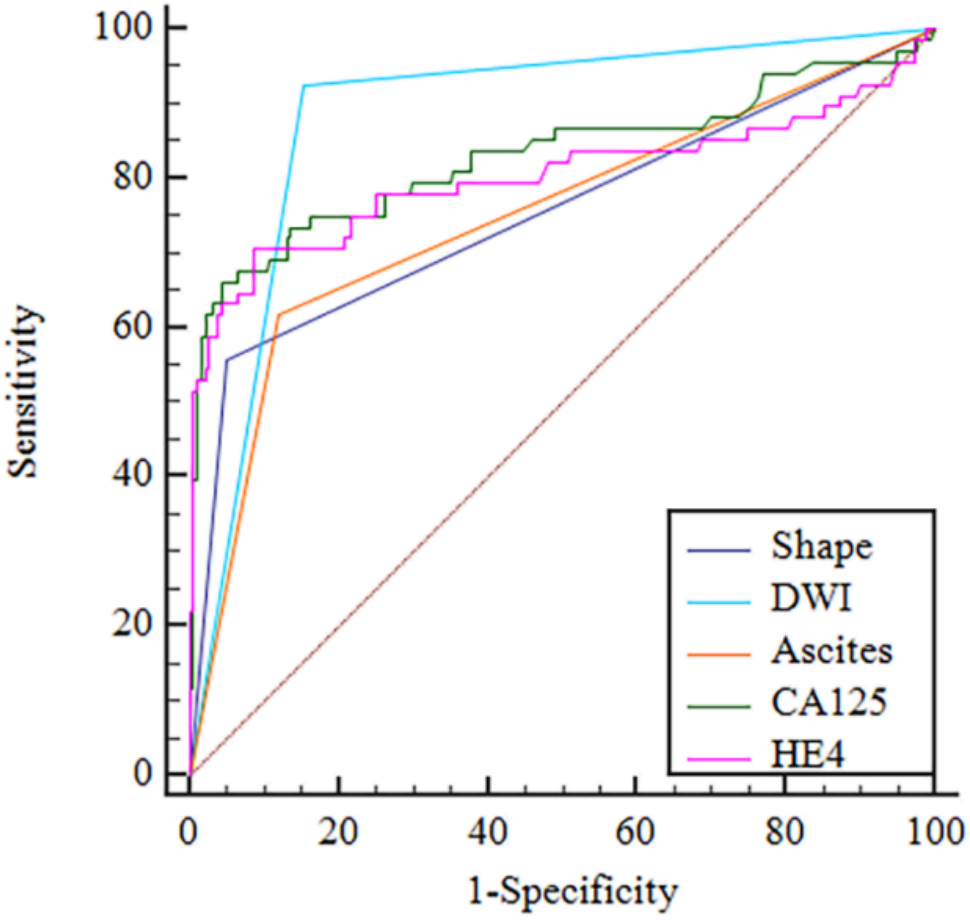

Figure 1

ROC curves of individual independent predictors for differentiating benign and malignant epithelial ovarian tumors. AUC values are indicated for each variable.

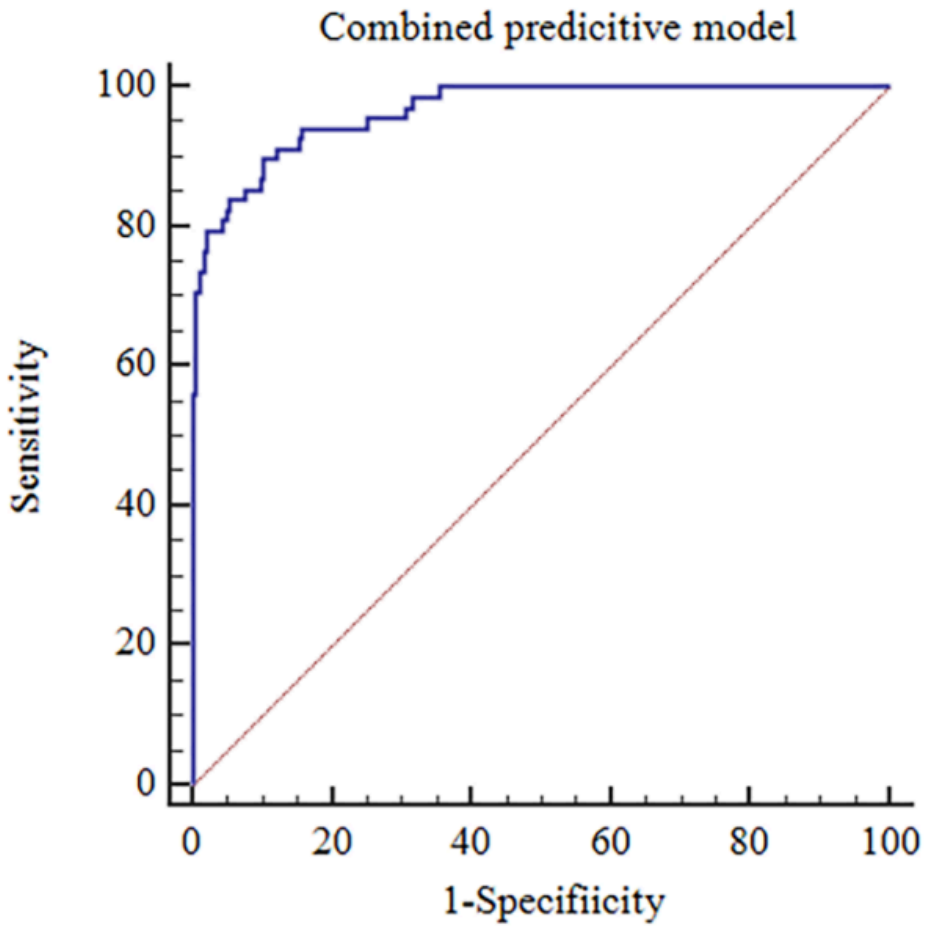

Figure 2

ROC curve of the combined predictive model in the training cohort. The model demonstrates high discriminative ability for distinguishing benign from malignant epithelial ovarian tumors.

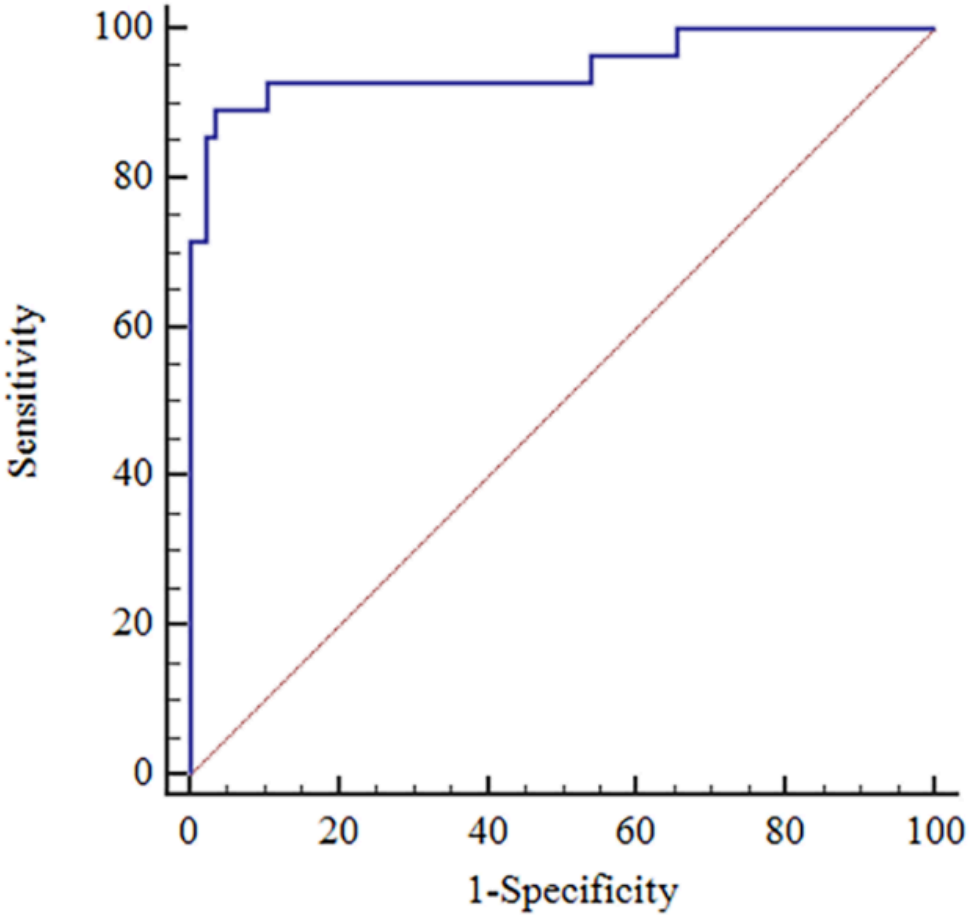

Figure 3

ROC curve of the combined predictive model in the external validation cohort. The model maintains excellent diagnostic performance across an independent patient cohort.

Supplementary Files

This is a list of supplementary files associated with this preprint. Click to download.

- rawdata.xlsx